DETECTION OF BONDLINE DELAMINATIONS IN MULTILAYER STRUCTURES WITH LOSSY COMPONENTS†

ERIC I. MADARAS, WILLIAM P. WINFREE,
B.T. SMITH*, and JOSEPH H. HEYMAN

NASA Langley Research Center, Hampton, Va. 23665
*Physics Department, Christopher Newport College,
Newport News, Va. 23606

ABSTRACT

The detection of bondline delaminations in multilayer structures using ultrasonic reflection techniques is a generic problem in adhesively bonded composite structures such as the Space Shuttle's Solid Rocket Motors (SRM). Standard pulse echo ultrasonic techniques do not perform well for a composite resonator composed of a resonant layer combined with attenuating layers. Excessive ringing in the resonant layer tends to mask internal echoes emanating from the attenuating layers. The SRM is made up of a resonant steel layer backed by layers of adhesive, rubber, liner, and fuel, which are ultrasonically attenuating. The structure's response is modeled as a lossy ultrasonic transmission line. The model predicts that the acoustic response of the system is sensitive to delaminations at the interior bondlines in a few narrow frequency bands. These predictions are verified by measurements on a fabricated system. Successful imaging of internal delaminations is sensitive to proper selection of the interrogating frequency. Images of fabricated bondline delaminations are presented based on these studies

I. Introduction

NASA has set a goal of testing the Space Shuttle system for safety and reliability as completely as possible. The Rogers Commission Report indicated that detection of delaminations at the bondlines is an important component of quality assurance for the solid rocket motors (SRM). The SRM is made up of a thick steel layer backed by several layers of adhesives, rubber, liners, and fuel, which are ultrasonically attenuating. Standard pulse echo ultrasonic techniques are insufficient to perform the testing reliably on motors from the preferred steel side to avoid the sensitive fuel. The ultrasonic inspection of this structure is compromised by the excessive "ringing" of the steel when acoustically pulsed. This is a generic problem when a high acoustic "Q" layer is bonded to lossy, low acoustic "Q" layers. The echoes from the steel layer last for a significant amount of time, overlapping and interfering with the weaker echoes from the rubber, liner and fuel. These weaker echoes are only a few percent or less in amplitude of the larger steel interface echoes. Our approach is to model the SRM structure as a lossy ultrasonic transmission line. The model calculations provide the starting point to determine which are the best ultrasonic parameters to measure for detecting delaminations at the bondlines. From this treatment one can then try to devise testing techniques that will be robust when applied to actual hardware.

†This work was supported in part by NASA grant NAG-1-431

Testing on actual hardware is difficult and inconvenient because of size and weight considerations (twelve foot diameter motor segments weigh about 250 thousand pounds when loaded) and the expense of relocating equipment and personnel at the production facility. For this reason, Morton Thiokol manufactured laboratory size samples that were more manageable. These samples were built to closely approximate the actual construction of an SRM system and incorporated defects to allow us to test various methods.

II. Theory

To model the SRM sample, a normal incident acoustic wave was assumed to be propagating from a semi-infinite media to a layered system. The reflection of the front of the layer system is given by the expression

$$R = (Z_{1\_N} - Z_0) \; / \; (Z_{1\_N} + Z_0) \qquad (1),$$

where Z_0 is the acoustic impedance of the semi-infinite media and Z_{1_N} is the acoustic impedance of the entire set of layers from 1 to N. The acoustic impedance of the layered system can be found from the expression [1,2]

$$Z_{i\_N} = (Z_i + Z_{i+1\_N} \tanh(\theta_i d_i)) \; / \; (Z_{i+1\_N} + Z_i \tanh(\theta_i d_i)) \qquad (2),$$

where Z_{i+1_N} is the acoustic impedance of the set of layers from layers i+1 to N, Z_i, d_i are the the acoustic impedance and thickness of the i^{th} layer, and θ_i is given by the expression

$$\theta_i = \alpha_i + i\omega/c_i \qquad (3),$$

where c_i and α_i are the acoustic velocity and attenuation of the i^{th} layer. Equation (2) is used initially to solve for the impedance of the

N-1 layer and then successively applied until i is equal to 1. The result is substituted into equation (1) to find the reflection from the layered system.

To isolate the effect of layers 2 to N, the experimental procedure typically does not gate in the echo from the front face of the first layer. To simulate this in the model the reflection coefficient for the semi-infinite media backed by a semi-infinite first layer is subtracted from the results giving,

$$R = (Z_{1\_N} - Z_0) / (Z_{1\_N} + Z_0) - (Z_1 - Z_0) / (Z_1 + Z_0) \qquad (4).$$

Equation (4) can then used to calculate the spectral response of different layer configurations.

Typical acoustical responses for a steel, insulation, liner, inert fuel system with and without a disbond between the liner and fuel are shown in figure 1. The acoustic properties used to calculate the spectra are given in table 1. As can be seen from the figure, the most significant difference between the two spectra occurs at the peaks which correspond to the acoustic resonance of the steel layer. The figure also indicates the sign as well as the magnitude of the amplitude difference between the two spectra which depends on which steel resonance is chosen for investigation.

A similar effect is seen when varying the insulation thickness and finding the peak amplitude, which is shown in figure 2 for both the bonded and disbonded sample. The figure indicates that for most insulation thicknesses, there exist a difference in the amplitude of this peak. However, the contrast between the disbonded and bonded condition goes from positive to negative for some insulation thickness. Therefore, discrimination of disbonded from bonded regions requires an accurate knowledge of the thickness of the different layers. The samples fabricated for our investigation have insulation thicknesses of 0.0025 m and 0.0127 m. For the thinner insulation the contrast is negative, however for the thicker insulation the contrast is positive at the first steel resonance. The figure also indicates for some thicknesses, no difference exists in the peak amplitude between the bonded and disbonded case. Then the additional use of frequency information may be required to help resolve the disbond.

Table 1
Acoustic Material Properties of SRM Components

Material	Velocity m/sec	Density kg/m^3	Attenuation nepers/m
Steel	6080	7600	0
Insulation	1810	1218	$1.11 \times 10^{-5} f^{1.225}$
Liner	1500	999	$23.0\ f^{0}$
Fuel	2170	1503	$213.\ f^{0}$

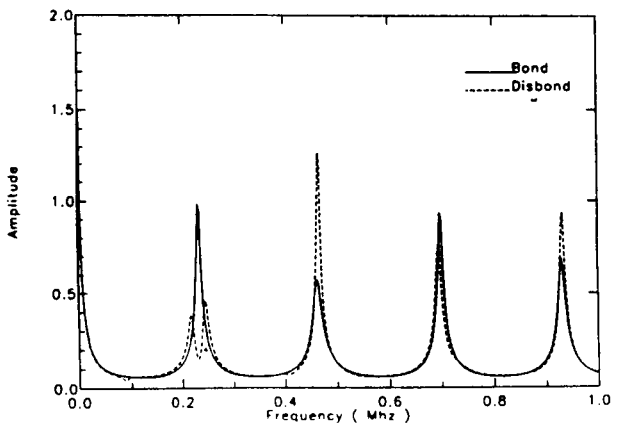

Figure 1. Calculated spectral response of a layered SRM system comparing a normal bonded sample with 0.127 m of steel, 0.0025 m of insulation, .0025 m of liner and 0.1016 m of inert fuel vs. a disbond condition between the liner and fuel.

III. Samples

The samples used in this work were manufactured by Morton Thiokol, the manufacturer of the SRM systems for NASA. The samples were made to represent the SRM system's cross section as close as reasonably possible (see Fig. 3). To emulate a disbonded condition, thin brass wedge shaped shims were cured into the samples at various bondlines. The thin strips of metal extended beyond the sample's edge so that they could be withdrawn after cure to produce an obvious disbond. The

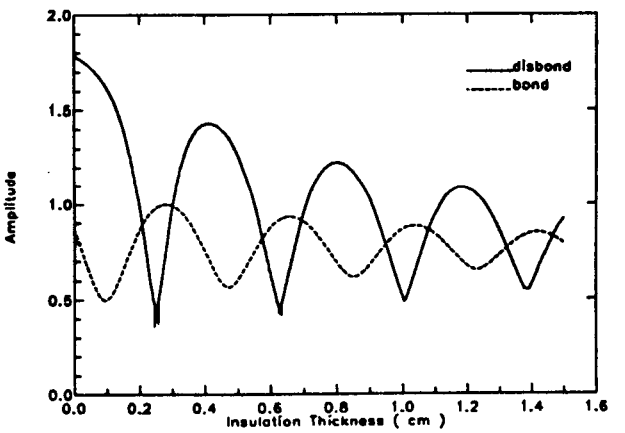

Figure 2. Calculated contrast levels at the first steel resonance of layered SRM system with varying thicknesses of insulation comparing a normal bonded sample with 0.127 m of steel, insulation, .0025 m of liner and 0.1016 m of inert fuel vs. a disbond condition between the liner and fuel.

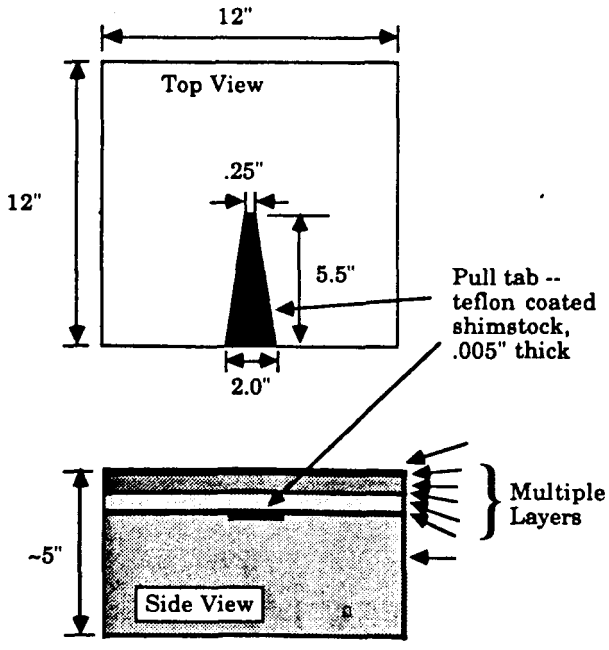

Fig. 3. Sample cross section of the SRM system.

samples were 12 inches by 12 inches square and had different thicknesses of the insulation materials that would go into manufacturing the motors (.0025 m and .0137 m) Fig. 3 shows an example of one of the samples. For safety, the fuel layer was rendered inert by replacing the oxidizer component with sodium chloride. The cross-sectional shape of the delaminations were identical in each sample.

Exposure to water would damage the liner and fuel on these samples. In order to use water as a couplant, we mounted plastic sides from a water tank to the top surface (steel side) of the SRM samples and attached the sides with a caulking compound (RTV). In this manner, the steel side of the sample became a water tight tank which we could scan using water as the couplant on the steel side and not compromise the fuel and insulation layers with moisture absorption. Since the samples had a small amount of curvature, a simple device was made that maintained the transducer perpendicular to the surface of the sample.

IV. Equipment

Using the results of the model calculations it is clear that the physical parameters of the ultrasonic wave interaction with the bondlines can be measured by many techniques. The methods though different rely on the same physics. Three techniques are illustrated here.

Figure 4 shows an outline of the electronic apparatus. The system shown in 4a used a spectrum analyzer to capture the spectral response of the sample to the ultrasonic signal. The spectrum analyzer's tracking generator output was attenuated and fed through a set of transmitter gates to the transmitter. The transmitter gate width was set for approximately a 40 microsecond long tone burst. This length of the tone burst was long enough to generate standing waves in the outer layers of the SRM sample. The ultrasound was coupled into the sample through a water delay line of approximately 70 microseconds long. A flat 500 KHz, 1.125" diameter broadband transducer was used for insonifying the sample. The echoes were then fed into a set of receiver gates to select the desired portion of the RF signals for input into the spectrum analyzer. The receiver gates sampled the RF signal from the tone burst's echo several microseconds after the sample's front surface echo had past but the interior echoes remained. The acoustic "Q" of the system is then being detected. The spectrum analyzer output was recorded on a microcomputer that also controlled a position scanner that allowed us to produce an image of the SRM sample's spectral response.

Figure 4b. shows a simple system that is based on a similar principle. A ten cycle tone burst at a frequency of 500 KHz (the second harmonic of the steel) was used. This tone burst was transmitted using a 500 KHz, 1.125" diameter planar transducer. The reflected signal was gated into the receiver just after the front wall echo had past and the gated signal was detected. The gated detector was also replaced with a waveform digitizer. Signal processing in the frequency and time domains was then applied to extract the physical parameter of interest. the results are similar and are not included in this work.

Figure 4c. demonstrates still a third system that we developed. This system is designed to track an ultrasonic resonance of the sample and measure both the amplitude and phase of the signal [3]. This is desirable if the thickness of the steel or deeper layers should change causing a phase shift in the signal. A slow sinusoidal signal is applied to the control port of a VCO causing the oscillator to FM the output. The echo of the transmitted tone burst is detected after the front wall echo has passed and the resulting signal is measured. The amplitude of the signal varies because of the frequency modulation and this variation is used to generate an error signal that is fed back into the VCO to keep the frequency at the peak of the resonance. In this manner, it could track both the amplitude and frequency of a resonant peak should a thickness change occur and cause the resonance to be different than anticipated.

V. Results

The spectral response of the sample which was convolved with the system's response showed several resonant structures and is shown in figure 5. The spectral response of these SRM samples should have resonances near 250, 500, and 750 KHz which are expected to arise from the 0.0127 m of steel. The general resonant structures that were related to

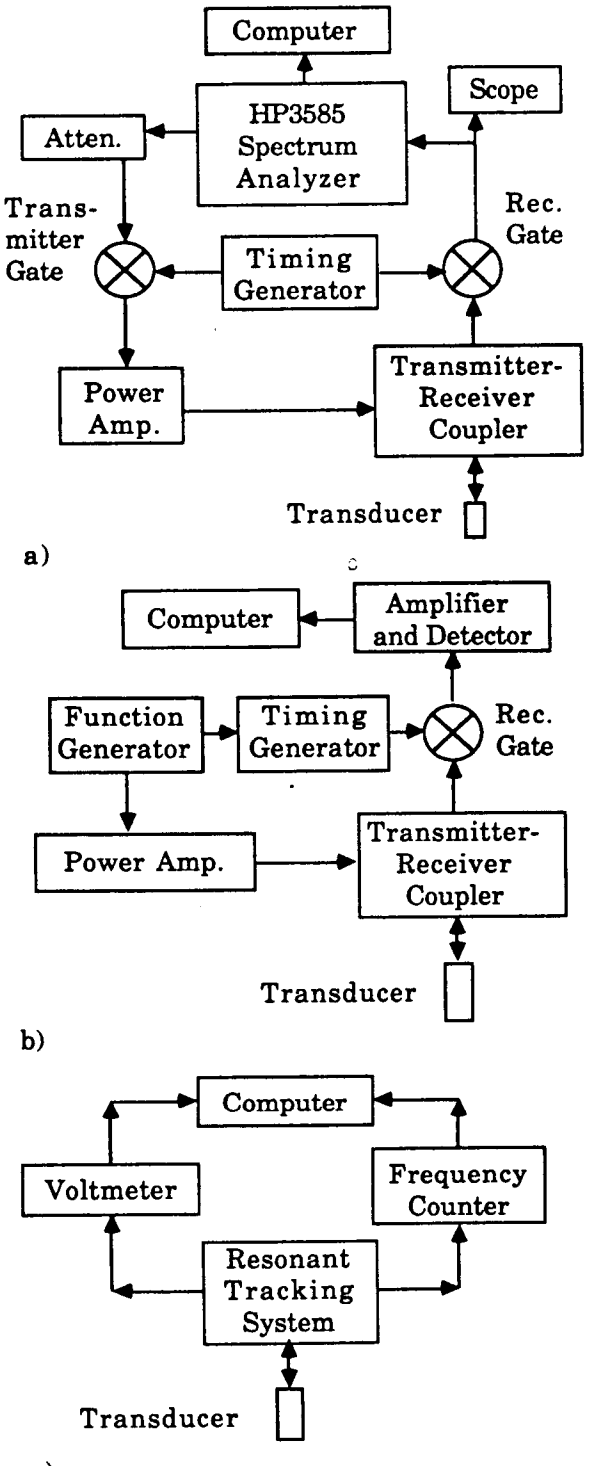

Fig. 4. three different systems used to view the samples with disbond regions.

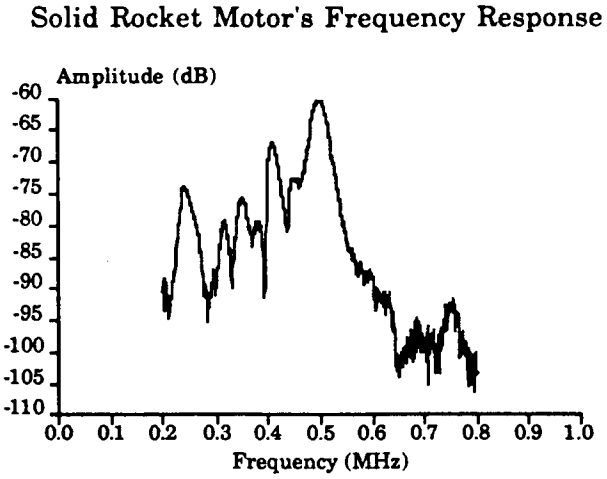

Fig. 5. The frequency response of the system to the SRM samples.

the theoretical predictions were evident. A few others resonances which were not of interest were evident and were possibly generated by side lobe effects or other modes. The 490 KHz resonance dominates because it is near the center frequency of the transducer. The rubber insulation will have less effects on the resonances at the higher frequencies because the attenuation of the rubber is frequency dependent. The rubber will also limit the penetration of the ultrasound and its ability to detail defects deeper into the material. Therefore, the lower frequencies are the most attractive for purposes of deeper interrogation.

Figure 6a. shows an image based on peak detecting a standard pulse echo system. The step size is 0.2 cm and the image size is 8 X 12 cm. The sample has 0.0025 m. of insulation behind the steel and the delamination is at the liner to fuel interface. The delamination is not resolved using this standard technique. These echoes are difficult to resolve in part because the ultrasonic energy is being transmitted over a wide band of frequencies, whereas the sample has a stronger response at the resonance frequencies. In contrast, figure 6b, shows the results of the tone burst system shown in figure 4b. This figure represents the same scan area as figure 6a. The delamination is now resolved by transmitting energy at a sensitive resonance. This image has the inverse contrast as predicted by theory. This is undoubtedly due to difficulties in laying up the samples. In particular, materials like the liner and fuel are viscous liquids when they are applied. In small samples, it can be difficult to maintain their thicknesses. Also, the cured liner material is fairly soft, and it would be easy to disturb its shape when the insert that creates the disbond is cured into the system

Figures 7a and 7b show the results of images based

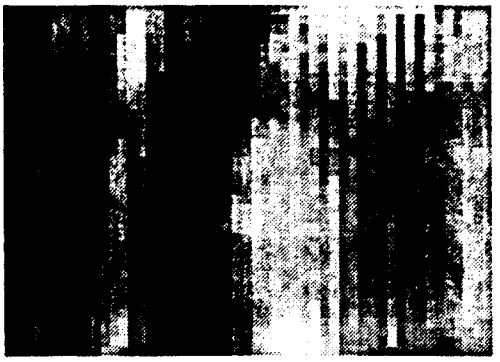

a)

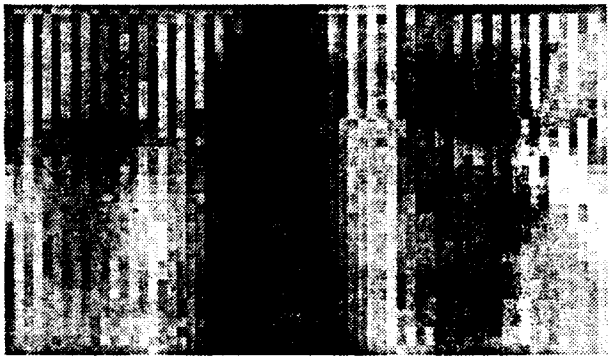

b)

Figure 6 Ultrasonic images of manufactured disbonds with 0.0025 m of insulation behind the steel. (a) Represents a standard peak detection system. (b) Represents a tone burst at the second steel harmonic resonance detected system.

on the first steel harmonic (~240 KHz) and the second steel harmonic (~490 KHz) using the technique based on the spectrum analyzer. The scans were from a 50 by 50 pixel scan with a 0.25 cm step size per pixel. This sample had 0.0137 m of insulation behind the steel with a disbond between the liner and fuel. The spectra were smoothed and the peak signal intensity near the desired frequency was selected. The image based on the first harmonic displayed the shape of the delamination reliably, with about a 2-3 dB increase in intensity at the disbond region. The contrast of the image is lost in the image based on the second harmonic and does not show the disbond region with as much reliably as the 240 KHz image. The second harmonic image is in a frequency range where the contrast is predicted to be poorer.

Figure 8 shows the results of imaging a sample, which has 0.0025 m of insulation behind the steel, with the system that would track the resonant frequency as well as the amplitude at the resonant peak. In this case, a frequency shift of the

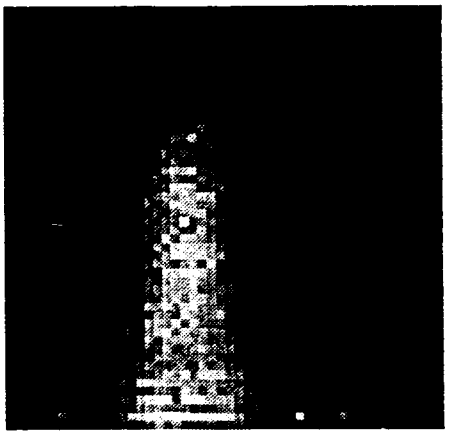

(a)

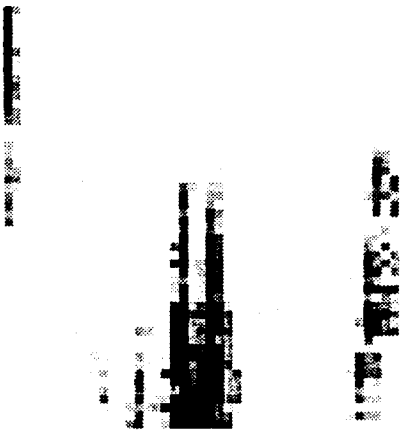

(b)

Figure 7. Ultrasonic images of manufactured disbonds with 0.0127 m of insulation behind the steel using system depicted in figure 4(a). (a) Represents the first steel harmonic resonance peak. (b) Represents the second steel harmonic resonance peak.

resonance is evident in figure 8b. This results in a very high contrast image in the frequency scan, and a lower contrast in the amplitude image. As was indicated in the theory section, the amplitude contrast may be small at the peak for some material thicknesses, and the addition of the frequency information could greatly help in the interpretation.

Each of the frequency selective techniques we tried showed the delamination regions. They each have their respective advantages and disadvantages. In the system shown in figure 4a, the use of the whole spectrum is very time consuming. It is helpful in demonstrating the model, but it

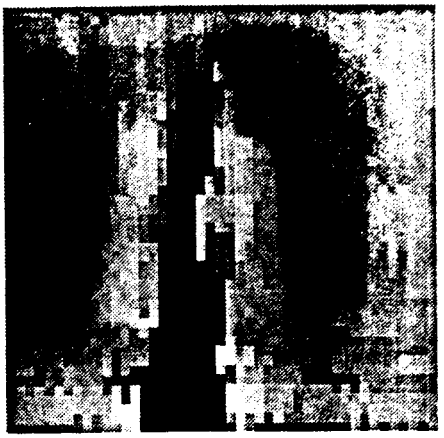

(a)

(b)

Figure 8. Ultrasonic images of manufactured disbonds with 0.0025 m of insulation behind the steel using system depicted in figure 4(c). (a) Represents the phase of the second steel harmonic resonance peak. (b) Represents the amplitude of the second steel harmonic resonance peak.

would not be practical in a production setting. The system depicted in figure 4b, is simple and quick, but the possibility of small shifts in frequency due to thickness changes in either the steel or deeper layers could cause false indications if one is not careful, especially with the added effects of the transducer response. The third system shown in figure 4c, is a compromise between the first two systems. In this system, care must be used in setting the frequency modulation level in case there are nearby resonances. It would be easy to jump to a different peak if the FM modulation is set high enough, and this could result in an image that would lose its significance.

VI. Conclusion

For systems such as the Solid Rocket Motor, large regions of the case are constructed of uniform layers of steel, insulation, liners and fuel. The curvature of the motor is large so that the layers can be approximated as nearly planar layers. For low frequencies, the wavelength of sound is long enough so that phase cancellation effects due to the curvature are not detrimental to ultrasonic testing. Under these conditions, the treatment of this layered system as an ultrasonic transmission line appears to be valid.

The ultrasonic model indicates that the best contrast can be obtained near resonances of the system. Our measurements show that this is true. Often the application of materials such as liners and adhesives are applied unevenly. Because of these possible variations in thickness, acoustic amplitude and phase will be important in helping to interpret measurements. Indications are that successful testing of some areas of the SRM should be attainable.

VII. Acknowledgments

The authors would like to acknowledge the assistance of Dale Stone and Mark Froggart in the construction of the "Pseudo Continuous Wave" instrument used in this experiment.

VIII. References

1. O'Donnell, M., Busse, L. J., and Miller, J. G., "Piezoelectric Transducers", Methods of Experimental Physics: Ultrasonics, Ed. Peter. D. Edmonds, vol. 19, pp 29-66, Academic Press, Inc. N. Y. (1981).
2. Brekhovskikh, L. M., Waves in Layered Media, Trans. by R. T. Beyer, Academic Press, Inc., N. Y. (1980).
3. Heyman, J. S., "Pseudo Continuous Wave Instrument", United States Patent 4,117,731, (1978).